A Short Review of the S_4 Symmetric Microscopic Model for Iron-Based High Temperature Superconductors

Jiangping Hu

Beijing National Laboratory for Condensed Matter Physics, Institute of Physics, Chinese Academy of Sciences, Beijing 100080, China & Department of Physics, Purdue University, West Lafayette, Indiana 47907, USA

E-mail: jphu@iphy.ac.cn & hu4@purdue.edu

Abstract. We briefly review the recently constructed two orbital microscopic model for iron-based superconductors based on S_4 symmetry[1]. With this faithful representation of the kinematics of the tri-layer FeAs or FeSe structure, the model provides answers and physical pictures to fundamental questions related to the robustness of superconductivity and pairing symmetry, unifies different families of iron-based superconductors, casts new insight into the connections to the other high T_c superconductors, cuprates, and reveals why an s-wave pairing can be stabilized by repulsive interactions. Further progresses include that the model provides a clean understanding of band reconstruction observed in magnetically ordered states, which is a strong support to the kinematics of the S_4 model, and captures the essential low energy physics of iron-based superconductors based on numerical results from unbiased quantum Monte Carlo simulation.

1. Introduction

In the past four years, the main theoretical difficulty in understanding iron-based high temperature superconductors[2, 3, 4, 5] stems from the fact that the materials are intrinsic multi-orbital systems due to the presence of all five 3d-orbitals of iron atoms. Several initial attempts to construct simplified models with fewer orbitals was made in an early stage of the research[6, 7, 8]. While these models could successfully explain some properties, they all had serious drawbacks, which resulted in a belief that any microscopic model composed of less than all five d-orbitals is insufficient[9, 10].

Recently, very surprisingly, with a proper consideration of the S_4 symmetry, the symmetry of the building block–the FeAs or FeSe trilayer, we demonstrate that an effective two-orbital model is sufficient to capture the kinematics responsible for low energy physics [1]. The two orbital model includes two nearly degenerate and weakly coupled single-orbital parts that can be mapped to each other under the S_4 transformation. Not only has the model greatly simplified kinematics which essentially can be described by only three important tight-binding hopping parameters, but the model also has manifested a clear physical picture to explore many intriguing fundamental properties of the materials and has drawn a deep connection to the other high temperature superconductors, cuprates. In this paper, we give a quick review of the model by emphasizing its unique aspects and summarizing recent numerical and analytic results[11, 12].

Content from this work may be used under the terms of the Creative Commons Attribution 3.0 licence. Any further distribution of this work must maintain attribution to the author(s) and the title of the work, journal citation and DOI.
Published under licence by IOP Publishing Ltd

2. Motivation

Before proceeding to the S_4 model, we discuss several main initial motivations which lead to the construction of the model. The motivations stem from a few intriguing questions related to iron-based superconductors.

- *What is the relation between iron-based superconductors and cuprates?* This question has undoubtedly been asked by many researchers since iron-pnictides were discovered. In the past several years, it has been shown that the two classes of materials share many similar properties, including similar layered lattice structures, phase diagrams, strong antiferromagnetism in parental compounds, short superconducting coherent lengths and so on. However, it is still highly controversial that whether iron-based superconductors allow us to finally apply the induction method for high temperature superconductors.
- *How can the two different families of iron-based superconductors, iron-pnictides and iron chalcogenides, be unified?* Iron-based superconductors include two families, iron-pnictides[2, 3, 4] and iron-chalcogenides[5]. They share many intriguing common properties. They both have the highest T_cs around 50K[13, 3, 14, 15, 16]. The superconducting gaps are close to isotropic around Fermi surfaces[17, 18, 19, 20, 21, 22] and the ratio between the gap and T_c, $2\Delta/T_c$, are much larger than the BCS ratio, 3.52, in both families. However, the electronic structures in the two families, in particular, the Fermi surface topologies, are quite different in the materials reaching the highest T_c. The hole pockets are absent in iron-chalcogenides but present in iron-pnictides[17, 20, 21, 22]. The presence of the hole pockets has been a necessity for superconductivity in the majority of studies and models which deeply depend on the properties of Fermi surfaces[9, 13, 23, 24, 25, 26, 27, 28, 29, 30]. Therefore, the absence of the hole pockets in iron-chalcogenides causes a strong debate over whether both families belong to the same category that shares a common superconducting mechanism.
- *Why and how can a s-wave pairing state be stabilized if the superconductivity is originated from a repulsive interaction?* With a d-wave pairing symmetry, such as in cuprates, the positive and negative signs of the superconducting order parameter are equally distributed in both real and reciprocal space . Therefore, one can argue that the onsite repulsive interaction is naturally avoided in a d-wave pairing state. For a s-wave pairing symmetry, even in a sign changed $s^{\pm}$ state[24], the argument can not be held in general. While many of us use repulsive interactions to obtain a s-wave pairing or $s^{\pm}$, in iron-pnictides, this fundamental problem is largely unaddressed theoretically.
- *Why is the superconductivity so robust and how can a single energy scale dominate in pairing gap functions in iron-based superconductors?* Observed by angle-resolved photoemission microscopy (ARPES), a very intriguing property in the SC states of iron-pnictides is that the SC gaps around optimal doping on different Fermi surfaces are nearly proportional to a simple form factor $cosk_x cosk_y$ in reciprocal space. This form factor has been observed in both 122[17, 31, 18, 32] and 111[33, 34] families of iron-pnictides. Just like the d-wave form factor $cosk_x - cosk_y$ in cuprates, such a form factor indicates that the pairing between two next nearest neighbour (NNN) iron sites in real space dominates. In a multi-orbital model, many theoretical calculations based on weak coupling approaches have shown that the gap functions are very sensitive to detailed band structures and vary significantly when the doping changes[9, 26, 27, 28, 29, 30]. The robustness of the form factor has been argued to favor strong coupling approaches which emphasize electron-electron correlation or the effective next nearest neighbour (NNN) antiferromagnetic (AF) exchange coupling J_2[35, 36, 37, 38, 39, 40, 41, 42] as a primary source of the pairing force. However, realistically, it is very difficult to imagine there is a single energy scale in local exchange interactions if a multi d-orbital model is considered.

In order to answer the above questions, it is clear that we have to identify microscopic parameters that control the essential physics of iron-based superconductors at low energy.

3. Gauge mapping between the symmetries of superconductivity pairing and kinematics

The idea to address the robustness of possible s-wave pairing in iron-based superconductors stems from a paper by Berg, Scalapino and Kivelson[42], where they showed that the s-wave pairing in a two leg-ladder model for iron-pnictides is equivalent to a d-wave pairing in a similar model of cuprates. The s-wave and the d-wave can be mapped by a simple gauge transformation. Although their idea was carried out in an one-dimensional model, they raised an indispensable general point for any dimensional model, that is, *the pairing symmetry and kinematics must be considered together*. In particular, in a system where the short range pairing dominates, the phases or the signs of superconducting order parameters can be exchanged with those of the local hopping parameters.

3.1. Gauge Mapping

A gauge mapping can be generally described as follows. Given a general Hamiltonian including a kinetic energy $\hat{H}_0$ and an interaction energy $\hat{H}_I$, we can perform a gauge mapping that changes the sign of local Fermionic operators, namely,

$$c_i \to (-1)^{\theta_i} c_i \tag{1}$$

where $\theta_i = 0$, or 1. It is clear that such a general gauge mapping can be described by an unitary operator $\hat{U}$. Under the mapping, the hopping terms in $\hat{H}_0$ can change the sign so that the kinetic energy Hamiltonian is changed. However, the eigenvalues of $\hat{H}_0$ are not changed since it is an unitary transformation. It is also easy to see that the interaction Hamiltonian $\hat{H}_I$, if it includes standard interaction terms, such as local density interaction, spin exchange interaction and so on, in general, is not changed under the gauge transformation. Therefore, under the mapping,

$$\hat{H} = \hat{H}_0 + \hat{H}_I \to \hat{H}' = \hat{U}^+ \hat{H} \hat{U} = \hat{H}'_0 + \hat{H}_I. \tag{2}$$

If the original Hamiltonian $\hat{H}$ has a superconducting ground state with an superconducting order parameter $< c_i c_j >= \Delta_{ij}$, the ground state of the new Hamiltonian $\hat{H}'$ must have $< c_i c_j >= (-1)^{\theta_i + \theta_j} \Delta_{ij}$. Therefore, if the pairing is rather local short range, it is possible to change order parameter symmetry by choosing a proper gauge mapping.

3.2. Gauge mapping between d-wave and extended s-wave pairing symmetries in cuprates

Let's use cuprates as an example to illustrate the point. For cuprates, the kinetic energy $\hat{H}_0$ is dominated by the nearest neighbour(NN) hopping in a square lattice, namely,

$$H_0 = -t \sum_{<ij>} c^+_{i\alpha} c_{j\alpha} + ... \tag{3}$$

where $< ij >$ represents the links between two NN sites, and the order parameter of the d-wave pairing symmetry in real space is also dominated by coupling two NN sites which is corresponding to the d-wave gap form $cosk_x - cosk_y$ in reciprocal space, namely,

$$< c_i c_{i+\vec{y}} >= - < c_i c_{i+\vec{x}} >= \Delta_0 \tag{4}$$

where $\vec{x}, \vec{y}$ are lattice unit vectors along x and y directions respectively. As shown in fig.1, if we set a gauge mapping as

$$c_{i\alpha} \to (-1)^{i_x} c_{i\alpha}, \tag{5}$$

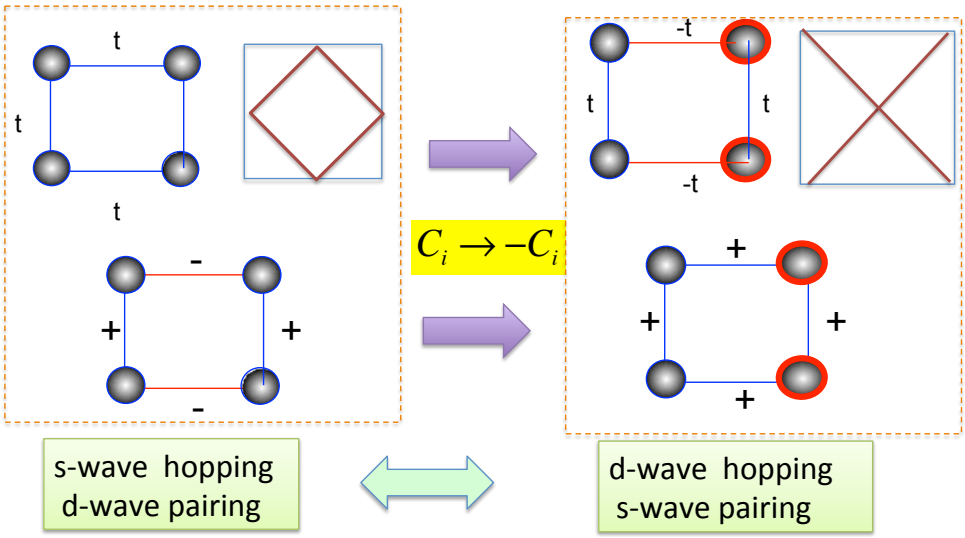

Figure 1. An illustration of the gauge mapping for cuprates. The left part of the figure shows the symmetry of the hopping parameters, d-wave pairing symemtry and the simplified Fermi surfaces at half filling. The right part shows their corresponding parts after the gauge mapping. The gague mapping changes the sign of Fermionic operators at the red sites.

where i_x labels the coordinate along the x direction of the ith site. After the mapping, we have

$$H_0' = -t \sum_{<ij>_y} c_{i\alpha}^{+} c_{j\alpha} + t \sum_{<ij>_x} c_{i\alpha}^{+} c_{j\alpha} \cdots \tag{6}$$

and

$$< c_i c_{i+\vec{y}} > = < c_i c_{i+\vec{x}} > = \Delta_0 \tag{7}$$

Therefore, the gauge mapping allows us to exchange the symmetries between the hopping parameters and the superconducting pairing order parameters. Before the gauge mapping, the hopping has a s-wave symmetry and the pairing has a d-wave symmetry. After the gauge mapping, the hopping has a d-wave symmetry and the pairing has a s-wave symmetry. It is also important to notice that the Fermi surface topology is changed after the gauge mapping as shown in fig.1. In a weak coupling approach, the Fermi surface topology has been the key ingredient to determine many properties, such as pairing symmetry. If the pairing is driven by repulsive interaction or antiferromagnetic fluctuations, the Fermi surface topology before the gauge mapping favors a d-wave symmetry while one can argue that the Fermi surface topology after the gauge mapping favors a s-wave symmetry. Therefore, the result obtained from a simple Fermi surface topology analysis is actually consistent with the gauge mapping result. We will revisit this point for iron-based superconductors in the following subsection.

3.3. Gauge mapping between extended s-wave and d-wave pairing symmetries in iron-based superconductors

The above analysis has been generalized to iron-based superconductors[1]. A similar gauge mapping which maps a s-wave to a d-wave pairing symmetry can be designed as shown in fig.2$(1, 2, 1', 2')$. We group four neighbour iron sites to form a super site and change the sign of Fermionic operators at the red iron sites in fig.2$(1')$. This transformation maps the A_{1g} s-wave $cos(k_x)cos(k_y)$ pairing symmetry in the original Fe lattice to a familiar d-wave $cosk_x' - cosk_y'$

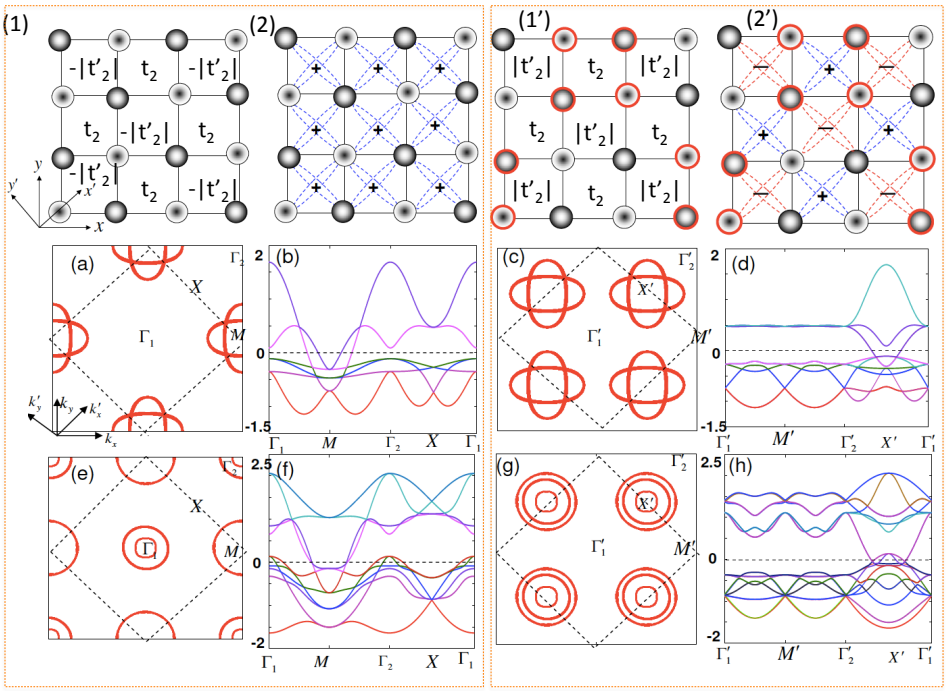

Figure 2. The illustration of the gauge mapping for iron-based superconductors: (1,2) and $(1', 2')$ sketch hopping parameters and pairing symmetries before and after the gauge mapping respectively; (a-h) band structures and Fermi surfaces for two models[36, 10] before and after the gauge mapping: (a,e) the Fermi surfaces, (b,f) the band dispersion along the high symmetry lines, (c,g) the Fermi surfaces after the gauge transformation, (d,h) the band dispersions along the high symmetry lines after the gauge transformation. The hopping parameters can be found in the above two references.

pairing symmetry defined in the two sublattices of the orginal lattice, where (k_x, k_y) and (k'_x, k'_y) label momentum in Brillouin zones of the origin lattice and sublattice respectively. This is actually a straightforward generalization of the transformation used in the study of the one dimensional iron ladder model[42].

Following the same procedure, we can ask how the kinetic energy changes. In ref.[1], we have shown that all the different tight binding models constructed for iron-based superconductors, after the gauge mapping, display very striking simplicity: (1) all Fermi surfaces after the gauge mapping are relocated around X', the anti-nodal points in a standard d-wave superconducting state in the sublattice Brillouin zone; (2) the bands previously located at the different places are magically linked in the new gauge setting. In particular, the two bands that contribute to electron pockets are nearly degenerate and the bands that contribute to hole pockets are remarkably connected to the former ones.

The first feature seriously challenges the consistency of previous weak coupling analysis depending on the difference of Fermi surface topologies for iron-pnictides and iron-chalcogenides. After the gauge mapping, based on the new Fermi surface topology, a standard weak coupling analysis would naturally favor a robust d-wave superconducting state with respect to the sublattice in the presence of repulsive interaction or NN AF coupling[43, 38]. Therefore, as shown in fig.3, if we reversely map to the original gauge setting, the original Hamiltonian must have a robust s-wave pairing symmetry. Namely, based on the new Fermi surface topology, both

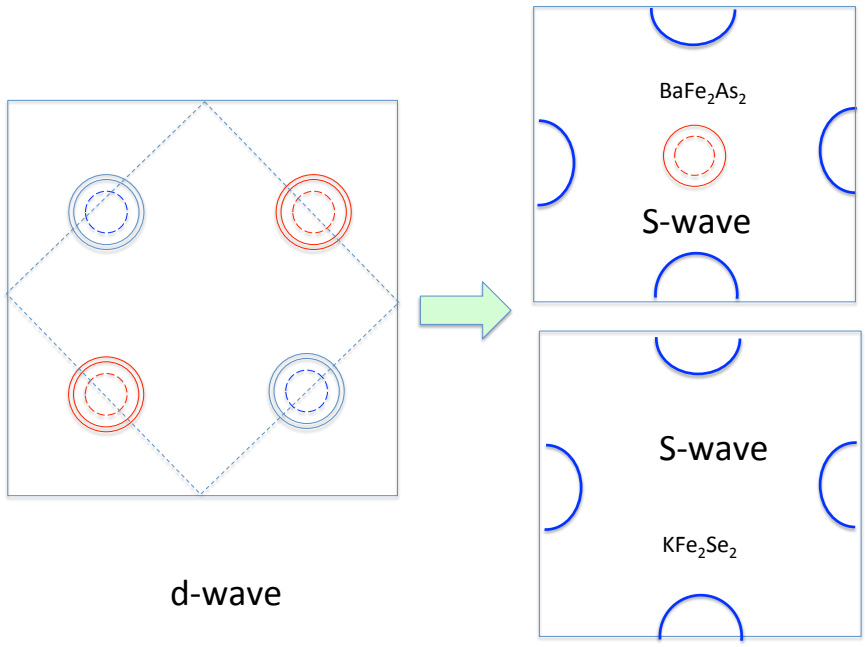

Figure 3. A sketch of a reverse gauge mapping from d-wave to s-wave for both iron-pnictides and iron-chalcogenides.

iron-pnictides and iron-chalcogenides should have s-wave pairing symmetry before the gauge mapping as long as the Fermi pockets are small.

The second feature is the key feature that leads us to believe that the low energy physics is controlled by a two orbital model which is characterized by two nearly degenerate bands. The emergence of the universal kinematics in different models suggest that the underlining electronic dynamics should be controlled by a much simplified set of parameters.

4. The construction of a two-orbital model with the S_4 symmetry

With above observations and the following important facts in the tri-layer FeAs or FeSe structure,

- The d-orbitals that form the bands near the Fermi surfaces are strongly hybridized with the p-orbitals of As(Se). Since the $d_{x'z}$ and $d_{y'z}$ have the largest overlap with the $p_{x'}$ and $p_{y'}$ orbitals, it is natural for us to use $d_{x'z}$ and $d_{y'z}$ to construct the model;
- The local lattice symmetry at an iron site is D_{2d} in which S_4 symmetry is the key symmetry operation;
- The two As(Se) planes are separated in space along c-axis in the tri-layer structure. Since there is little coupling between the p orbitals of the two planes and the hopping integrals through the p-orbitals are expected to dominate over the direct exchange couplings between the d-orbitals themselves, the two orbital model essentially could be decoupled into two nearly degenerate one orbital models;
- The decoupling must be controlled by the S_4 symmetry since S_4 symmetry links two As(Se) planes;

we draw a natural conclusion that the two-orbital model should be classified according to the S_4 symmetry and each of the two nearly degenerate one-orbital models should have a unit cell with

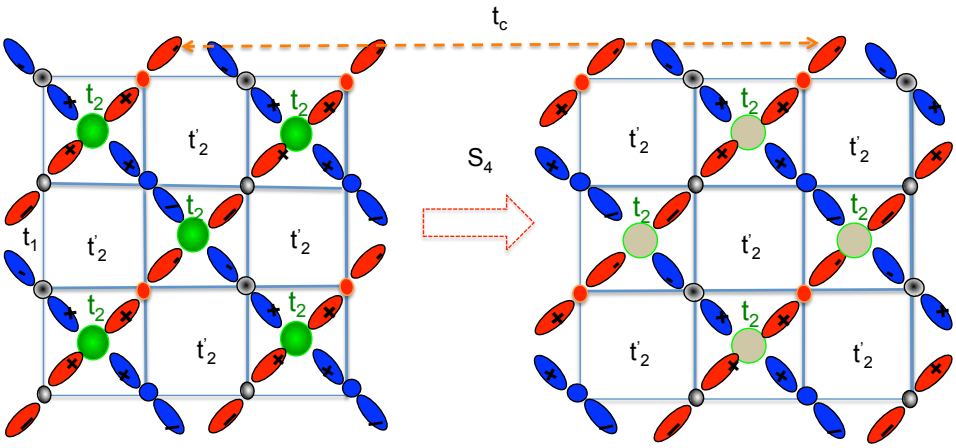

Figure 4. A sketch of the S_4 kinematics with $d_{x'z}$ and $d_{y'z}$ orbitals. The green balls represent As(Se) in the top layer and the grey balls represent those in the bottom layer. The blue and red orbitals represent the $d_{x'z}$ and $d_{y'z}$ orbitals.

two iron sites. A picture of the effective two-orbital model with the S_4 symmetry is illustrated in fig.4. The two orbital model is divided into two weakly and coupled one-orbital models. The orbital degree of freedom in the two one-orbital models can be called as two components of an S_4 iso-spin. The first one includes the $d_{x'z}$ in the A sublattice and the $d_{y'z}$ in the B sublattice if we use A and B to label two sublattices, and the second one includes the $d_{x'z}$ in the B sublattice and the $d_{y'z}$ in the A sublattice. The first strongly couples to the top As(Se) layer and the second couples to the bottom As(Se) layer. We denote $\hat{c}_{i\sigma}$ to $\hat{d}_{i\sigma}$ to label Fermionic operators of the two models that are connected by the S_4 transformation. Then, a general Hamiltonian that describes the kinematics is given by,

$$\hat{H}_{0,S_4} = \hat{H}_0 + \hat{H}_{0,c}, \tag{8}$$

where H_0 includes the two decoupled one-orbital models and $H_{0.c}$ which also obey the S_4 symmetry describes the weak coupling between the two models. As shown in[1], if we keep the leading hopping parameters,

$$\begin{aligned}\hat{H}_0 \quad = \quad & \sum_{k\sigma}[4t_{2s}cosk_x cosk_y - \mu](\hat{c}^+_{k\sigma}\hat{c}_{k\sigma} + \hat{d}^+_{k\sigma}\hat{d}_{k\sigma}) \\ & +2t_1(cosk_x + cosk_y)(\hat{c}^+_{k\sigma}\hat{c}_{k\sigma} - \hat{d}^+_{k\sigma}\hat{d}_{k\sigma}) \\ & +2t_{1d}(cosk_x - cosk_y)(\hat{c}^+_{k\sigma}\hat{c}_{k\sigma} + \hat{d}^+_{k\sigma}\hat{d}_{k\sigma}) \\ & +4t_{2d}sink_x sink_y(\hat{c}^+_{k\sigma}\hat{c}_{k+Q\sigma} - \hat{d}^+_{k\sigma}\hat{d}_{k+Q\sigma}) \\ & +2t_3(cos2k_x + cos2k_y)(\hat{c}^+_{k\sigma}\hat{c}_{k\sigma} + \hat{d}^+_{k\sigma}\hat{d}_{k\sigma}) \\ & +...\end{aligned} \tag{9}$$

and

$$\hat{H}_{0,c} = \sum_k 2t_c(cosk_x + cosk_y)(\hat{c}^+_{k\sigma}\hat{d}_{k\sigma} + h.c.). \tag{10}$$

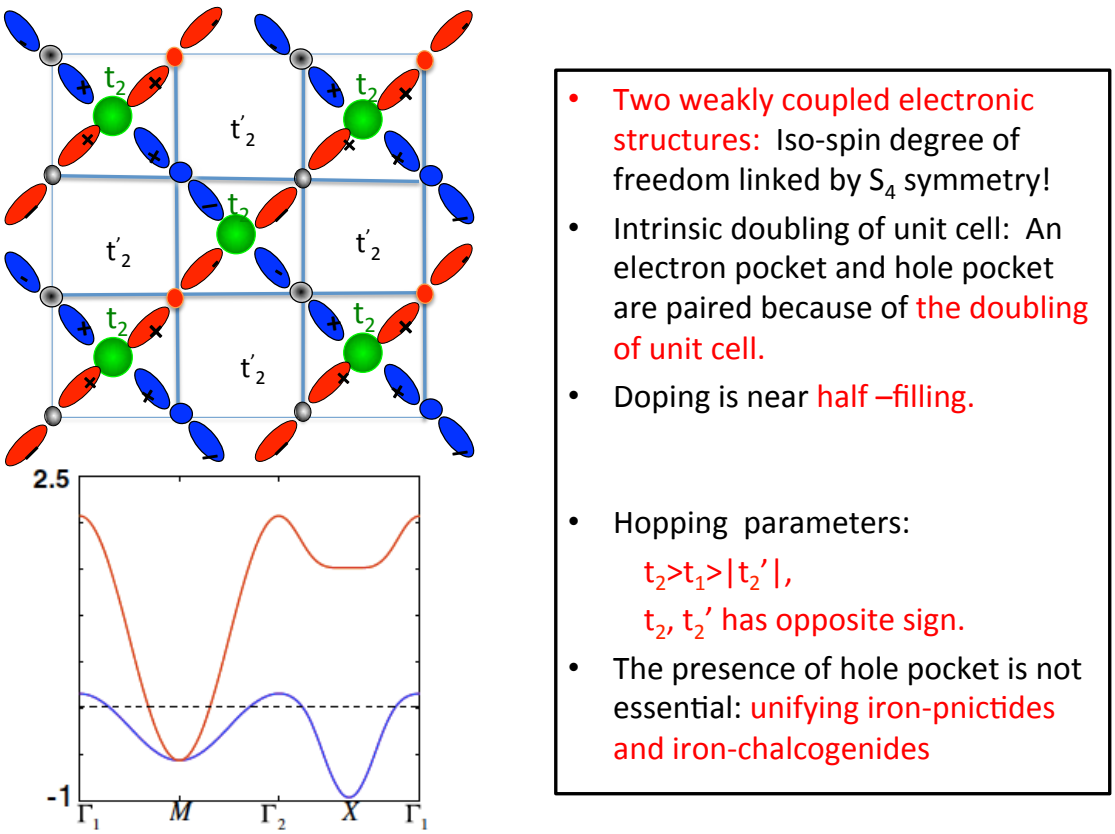

Figure 5. A sketch of the underlining kinematics and band structure of the S_4 model, and a list of the unique and important properties of the model.

where we limit the hopping parameters up to the third NN (TNN), including NN hoppings, t_{1x}, t_{1y}, NNN hoppings, t_2, t_2', and TNN hoppings, t_3. The longer range hoppings can be included if needed. For convenience, we have defined $t_{1s} = (t_{1x}+t_{1y})/2$, $t_{1d} = (t_{1x}-t_{1y})/2$, $t_{2s} = (t_2+t_2')/2$ and $t_{2d} = (t_2 - t_2')/2$.

Ignoring t_c, each S_4 iso-spin components provides the following two paired band energy dispersions due to unit cell doubling,

$$E_e = \epsilon_k + 4\sqrt{t_{2d}^2 sin^2 x sin^2 y + [\frac{t_{1s}(cosk_x + cosk_y) \pm t_{1d}(cosk_x - cosk_y)}{2}]^2}, \quad (11)$$

$$E_h = \epsilon_k - 4\sqrt{t_{2d}^2 sin^2 x sin^2 y + [\frac{t_{1s}(cosk_x + cosk_y) \pm t_{1d}(cosk_x - cosk_y)}{2}]^2}, \quad (12)$$

where $\epsilon_k = 4t_{2s}cosk_x cosk_y + 2t_3(cos2k_x + cos2k_y) - \mu$. E_e can capture the electron pocket at M points and E_h can capture the hole pocket at Γ point. t_{1s}, t_{2s} and t_{2d} are the key parameters. By just keeping these three parameters, the model is already good enough to capture the main characters of the bands contributing to the Fermi surface. Including interactions, the general

Hamiltonian is given by

$$H = H_{0,s_4} + U \sum_{i,\alpha=1,2} \hat{n}_{i,\alpha\uparrow}\hat{n}_{i,\alpha\downarrow} + U' \sum_i \hat{n}_{i,1}\hat{n}_{i,2} + J'_H \sum_i \hat{S}_{i,1} \cdot \hat{S}_{i,2} \tag{13}$$

where $\alpha = 1, 2$ labels the S_4 iso-spin, U describes the effective Hubbard repulsion interaction within each iso-spin, U' describes the one between them and J'_H describes the effective Hund′s coupling. Since the two components couple weakly, we may expect U dominates over U' and J'_H. Then, in the first order approximation, the model could become a single orbital-Hubbard model near half-filling.

In the original paper[1], we have suggested that t_{1s} breaks D_{2d} symmetry. This statement is not absolutely correct because t_{1s} and t_{1d} can be exchanged by choosing different orbital configurations. With the orbital configuration shown in fig.4, t_{1s} does not break D_{2d} symmetry. It is also important to note that the Γ point and the (π, π) point in Brillouin zone here are exchangeable because of the doubling of the unit cell.

5. Numerical results and supporting experimental evidence for the S_4 model

In fig.5, we summarize the important properties in the S_4 model. These properties include

- For each S_4 iso-spin, there is a pair of bands generated by unit cell doubling: one contributes a hole pocket and the other contributes an electron pocket.
- For each S_4 iso-spin, the filling factor is close to half-filling, an important property to allow strong spin fluctuation.
- The unit cell is intrinsically doubled, which is a very different starting point of kinematics from previous models.
- The hole pockets can be suppressed by adjusting t_{1s} or t_{2s}. Fixing t_{2d} and t_{2s}, reducing t_{1s} leads to flatter dispersion of the band responsible for the hole pockets. Thus, it suppresses the hole pockets. Therefore, the model unifies iron-pnictides and iron-chalcogenides.
- From orbital configuration, we have $t_2 > |t_{1s}| > |t'_2|$ and the signs of t_2 and t'_2 are opposite.

These characters have important physical consequences. In the following, we discuss some recent progresses associated with them.

5.1. Quantum Monte Carlo (QMC) Simulation on the S_4 model

The microscopic understanding provides a new opportunity to make use of highly controllable and unbiased numerical methods to study iron-based superconductors. In a recent paper[11], we have demonstrated that the model in the presence of electron-electron interaction is characterized by strong $(0, \pi)$ collinear antiferromagentic (C-AFM) fluctuations as observed in iron-based superconductors[44, 45, 46]. Moreover, the pairing with an extended s-wave symmetry robustly dominates over other pairings at low temperature in reasonable parameter region regardless of the change of Fermi surface topologies, namely, the presence or absence of hole pockets at Γ point. For both iron-pnictides and iron-chalcogenides, the pairing correlation, the effective pairing interaction and the antiferromagnetic correlation strongly increase as the on-site Coulomb interaction increases.

QMC results are summarized in fig.6. The competition between the s-wave and the d-wave in the S_4model is manifested by t_1 and t_2 where t_1 favors the d-wave while t_2 favors the s-wave. A simple phase diagram from QMC simulation is given as the inset in fig. 6(b). For iron-based superconductors, t_1 should be roughly equal to $t_2/2$ and $|t'_2|$ is much smaller than t_1 and t_2. Therefore, the s-wave should be robustly favored.

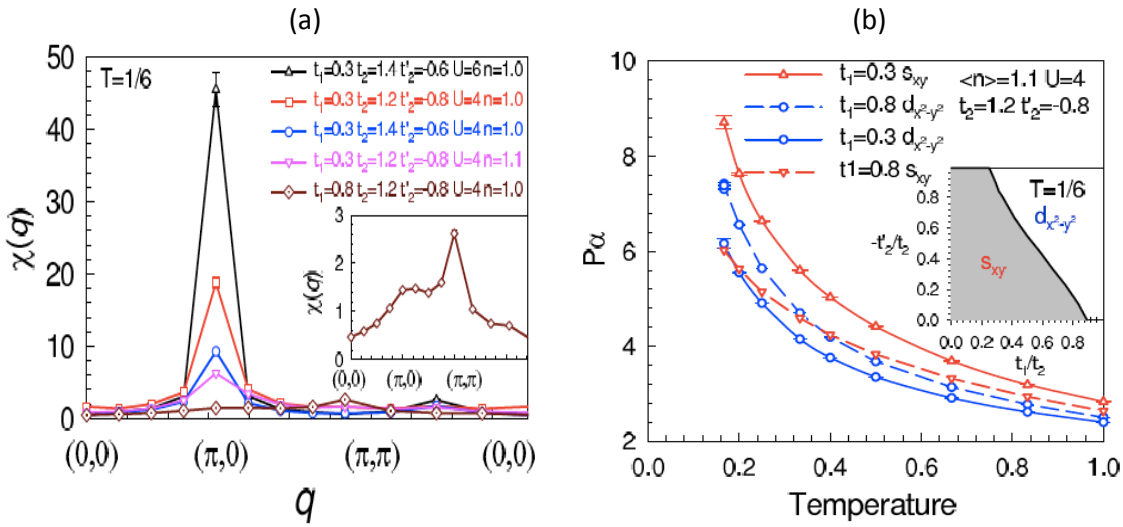

Figure 6. (a) Quantum Monte Carlo calculations about the static spin susceptibility for the S_4 model. The inset shows a significant large t_1 can change the peak from $(0, \pi)$ to (π, π), which signals the competition between NN hopping and NNN hopping. (b) The effective pairing interaction as a function of temperature at $< n >$=1.1, $U = 4.0$, $t_2 = 1.2$, $t_2' = -0.8$ for different t_1. Inset: the competition between s_{xy} and $d_{x^2-y^2}$ depends on t_1/t_2 and $-t_2'/t_2$.

5.2. Oriented gap opening in the C-AFM state: an impact of intrinsic unit cell doubling

As we have discussed above, one unique feature in the S_4 symmetry construction is that the unit cell includes 2 irons. Most of previous studies are based on models with one iron per unit cell. In principle, one can argue that models based on both representations should be equivalent. However, since the search of a meanfield result depends on the starting point of kinematics, a proper starting point is crucial to obtaining a correct meanfield result.

In a recent paper, we have demonstrated an important impact of the intrinsic unit cell doubling[12]. Unlike in a conventional spin density wave (SDW) state where gaps at any two points on the Fermi surface that are connected by the ordered SDW wave vector should be opened, the band structure in the C-AFM state appears to be reconstructed by the development of the magnetic order. ARPES experiments [47, 48, 49, 50, 51, 52] observe that small pockets or hot spots develop around Fermi surfaces. It is fair to say that the scenario of the gap opening due to a magnetic order in a multi-orbital system, such as iron-pnictides, is complex. For example, it has been argued that the entire Fermi surfaces can be gaped out[53]. Nevertheless, the surprising band reconstruction is never fully understood in previous models.

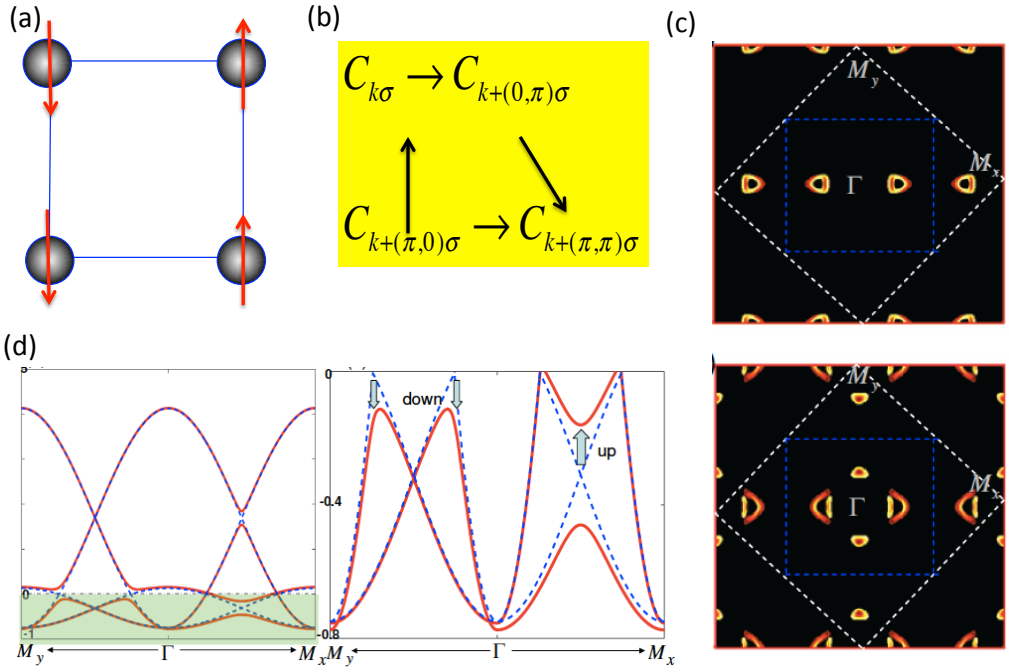

Figure 7. The illustration of oriented gap opening in magentically ordered state of iron-based superconductors: (a) The C-AFM magnetic state; (b) The illustration of the connections of four Fermionic operators in reciprocal space by the C-AFM order; (c) The typical Fermi surfaces in the C-AFM state; (d) The band reconstruction and gap opening in the C-AFM state.

As summarized in fig.7, the complicated band reconstruction near Fermi surfaces in the magnetically ordered state of iron-pnictides observed by ARPES can be understood in a meanfield level by the S_4 model. The $(0,\pi)$ or $(\pi,0)$ C-AFM order does not open gaps between two points on theFermi surfaces linked by the ordered wave vector but forces a band reconstruction involving four points in unfolded Brillouin zone and gives rise to small pockets or hot spots.

The doubling of the unit cell leads to an orientation-dependent gap opening in reciprocal space. In one $\Gamma - M$ direction, the magnetic order splits two folded bands while in the other direction the gap can be opened between the pair of electron and hole pocket bands. Such an oriented gap opening generates the hot spots or small pockets as observed by ARPES as shown in fig.7(c)..

5.3. Sign change between the top and bottom As(Se) planes in the s-wave state

The NNN hopping parameters t_2 and t_2' have opposite signs in the S_4 model. This sign difference stems from the orbital symmetries. If we take the gauge mapping mentioned earlier, after the mapping, the two hopping parameters in the new model have the same signs. Therefore, the gauge mapping exactly switches the symmetries between the pairing and the underlining

properties	iron SCs	cuprates
pairing symmetry	s-wave	d-wave
underlining hopping symmetry	d-wave	s-wave
dominant pairing form	$cosk_x cosk_y$	$cosk_x - cosk_y$
pairing classification symmetry	S_4	C_{4v}
unit cell	2 Fe (doubled)	1 Cu
AF coupling	NNN J_2	NN J_1
sign change in real space	c-axis	a-b plane
filling density	half-filling	half-filling

Table 1. A list of the close connections between iron-based superconductors (iron SCs) and cuprates.

kinematics as shown in fig.2$(1, 2, 1', 2')$.

In the view of the d-wave picture after the gauge mapping, the superconducting phase for each S_4 iso-spin alternates between neighboring squares, which is corresponding to the sign change between the top and bottom As/Se planes in the view of the S_4 symmetry. Such an intrinsic sign change between the top and bottom As planes along c-axis explains why a s-wave before gauge mapping can be stabilized even if the repulsive interaction is responsible for superconductivity.

The relative phase between the two S_4 iso-spins can take two different values, 0 or π, in principle. The difference can be classified as the irreducible representation of the S_4 symmetry. The S_4 point group has four one-dimensional representations, including A, B and $2E$. In the A state, the S_4 symmetry is maintained. In the B state, the state changes sign under the S_4 transformation. Therefore, in the A phase, since the S_4 symmetry is not violated, the relative phase between the two iso-spin are equal to π in space, while in the B phase, the relative phase is zero. The A phase in the presence of the hole pockets is an sign-changed s-wave or $s^{\pm}$ state. Therefore, the model predicts a new superconducting state, B phase state. However, it is still an open question whether iron-base superconductors can carry both states or not.

6. Discussion and perspectives

6.1. Comparison between cuprates and iron-based superconductors

By revealing the underlining electronic structure, we can make a close comparison between cuprates and iron-based superconductors. In Table.1, we list the close relations between two high T_c superconductors. From the table, it is clear that by determining these physical properties of iron-based superconductors listed in the table can help to determine the high T_c superconducting mechanism.

6.2. More supporting evidence for the S_4 symmetry

The S_4 model provides a microscopic understanding to two measured universal behaviors: the superconducting gap function that is dominated by the single $cosk_x cosk_y$ form and the almost universal NNN antiferromagnetic exchange coupling strength J_2 measured by neutron scattering[45, 54, 55] . The existence of such two single energy scale quantities is also a strong support for the S_4 model. If we treat the S_4 model in the presence of strong electron-electron correlation, both J_2 and the gap function in the s-wave state is determined by the NNN hopping parameters.

The S_4 model also suggests that the properties of an iron-based superconductor can be understood by simply observing bands responsible for electron pockets. Since the physics is dominated by the pair of bands that are responsible for a pair of hole and electron pockets. The

third hole pockets at the Γ point observed in iron-pnictides is not expected to play a significant role. However, the existence of the third hole pocket may change the doping concentration for the S_4 model in a stoichiometric material. Namely, in the view of the S_4 model, the material could be self electron doped. For example, if a large third hole pocket is present, we would expect that the S_4 model could be heavily electron-doped. This expectation naturally explains puzzled physical properties of $LiFeAs$ where a large third hole pocket was observed[56]. No static magnetic order is observed in the stoichiometric $LiFeAs$ with $T_c \sim 18K$[57, 58]. In the view of the S_4 model, the $LiFeAs$ is self electron doped so that many physical properties of the material should be understood from the heavy electron doped side of phase diagram[59].

6.3. Perspectives

The S_4 model provides a fresh starting point to explore novel physics in iron-based superconductors. Here, we discuss several perspectives for the future research.

First, since the S_4 symmetry stems from the fact that As stands out of Fe plane, obvious interesting physics may stem from c-axis coupling. Recently, ARPES has provided the existence of superconducting gap nodes along c-axis in $BaFe_2As_{2-x}P_x$[60, 61]. It is very likely that the S_4 symmetry may be linked to such a development of nodes since the superconducting phase along c-axis in the S_4 model has very intriguing sign change as we discussed earlier.

Second, electron nematism observed in iron-pnictides[62] can be fully investigated in the S_4 model. Namely, the S_4 model provides a microscopic base to understand electron nematism. The S_4 symmetry breaking can lead to an electron nematic state. In the previous theoretical studies, electron nematism is obtained through phenomenological models[63, 64, 65, 66].

Third, with only a set of three parameters describing kinematics, it becomes possible to obtain the dependence of these parameters on lattice parameters. Such an dependence may help us to explain empirical observations of the connection between the maximum T_cs and the As-Fe-As angles[13].

Fourth, it is interesting to investigate physical properties on surfaces where the S_4 symmetry, in principle, is naturally broken. A natural consequence of such a symmetry breaking is that symmetry broken states may be more stable on surfaces than in bulk.

Finally, the doping phase diagram and its parameter dependence, as well as many other physical quantities need to be investigated in the S_4 model.

6.4. Summary

The S_4 model provides great simplicity to study and unify the physics of iron-based superconductors. It reveals the deep connections between curpates and iron-based superconductors. Since the uniqueness of the model stems from the unique structure of FeAs or FeSe tri-layer, revealing such an underlining microscopic kinematics cast a new light on the search of new structures that can produce high superconducting transition temperatures.

7. Acknowledgments

The author acknowledges NN Hao, T. Ma, H. Lin, Y. Wang for collaborations and H. Ding, DL Feng, PC Dai, T. Xiang, X. Dai, S. Kivelson, D. H. Lee, F. Wang for useful discussions. The work is supported by the Ministry of Science and Technology of China 973 program(2012CB821400) and NSFC-1190024.

[1] Hu J and Hao N 2012 *Phys. Rev X* **2** 021009
[2] Kamihara Y, Watanabe T, Hirano M and Hosono H 2008 *J. Am. Chem. Soc.* **130** 3296
[3] Chen X H, Wu T, Wu G, Liu R H, Chen H and Fang D F 2008 *Nature* **453** 761
[4] Chen G F, Li Z, Wu D, Li G, Hu W Z, Dong J, Zheng P, Luo J L and Wang N L 2008 *Phys. Rev. Let.* **100**
[5] Guo J, Jin S, Wang G, Wang S, Zhu K, Zhou T, He M and Chen X 2010 *Phys. Rev. B* **82** 180520
[6] Daghofer M, Nicholson A, Moreo A and Dagotto E 2010 *Phys. Rev. B* **81** 14511
[7] Lee P A and Wen X G 2008 *Phys. Rev. B* **78** 144517

[8] Raghu S, Qi X L, Liu C X, Scalapino D J and Zhang S C 2008 *Phys. Rev. B* **77** 220503
[9] Hirschfeld P J, Korshunov M M and Mazin I I 2011 *Rep. Prog. Phys.* **74** 124508
[10] Kuroki K, Onari S, Arita R, Usui H, Tanaka Y, Kontani H and Aoki H 2008 *Phys. Rev. Lett.* **101** 087004
[11] Ma T, Lin H and Hu J 2012 *arXiv:1206.6277*
[12] Hao N N, Wang Y and Hu J 2012 *arXiv:1207.2798*
[13] Johnston D 2010 *Advances in Physics* **59** 803–1061
[14] Liu D and et al. 2012 *arXiv:1202.5849*
[15] Wang Q Y and et al. 2012 *arXiv:1201.5694*
[16] Sun L and et al. 2012 *Nature* **10.1038/nature10813**
[17] Ding H and et al 2008 *EPL (Europhysics Lett.)* **83** 47001
[18] Zhao L and et al. 2008 *Chin. Phys. Lett* **25** 4402
[19] Zhang Y, Yang L X, Chen F, Zhou B, Wang X F, Chen X H, Arita M, Shimada K, Namatame H, Taniguchi M, Hu J P, Xie B P and Feng D L 2010 *Phys. Rev. Lett.* **105** 1117003
[20] Wang X P, Qian T, Richard P, Zhang P, Dong J, Wang H D, Dong C H, Fang M H and Ding H 2011 *Europhysics Lett.* **93** 57001
[21] Zhang Y, Yang L X, Xu M, Ye Z R, Chen F, He C, Xu H C, Jiang J, Xie B P, Ying J J, Wang X F, Chen X H, Hu J P, Matsunami M, Kimura S and Feng D L 2011 *Nature Materials* **10** 273–277
[22] Mou D, Liu S, Jia X, He J, Peng Y, Zhao L, Yu L, Liu G, He S, Dong X, Zhang J, Wang H, Dong C, Fang M, Wang X, Peng Q, Wang Z, Zhang S, Yang F, Xu Z, Chen C and Zhou X J 2011 *Phys. Rev. Lett.* **106** 107001
[23] Dong J, Zhang H J, Xu G, Li Z, Li G, Hu W Z, Wu D, Chen G F, Dai X, Luo J L, Fang Z and Wang N L 2008 *Europhysics Lett.* **83** 27006
[24] Mazin I I, Singh D J, Johannes M D and Du M H 2008 *Phys. Rev. Lett.* **101** 57003
[25] Kuroki K, Onari S, Arita R, Usui H, Tanaka Y, Kontani H and Aoki H 2008 *Phys. Rev. Lett.* **101** 087004
[26] Wang F, Zhai H, Ran Y, Vishwanath A and Lee D H 2009 *Phys. Rev. Lett.* **102** 47005
[27] Thomale R, Platt C, Hu J P, Honerkamp C and Bernevig B A 2009 *Physical Review B* **80** 180505
[28] Thomale R, Platt C, Hanke W, Hu J and Bernevig B A 2011 *Phys. Rev. Lett.* **107** 117001
[29] Chubukov A V, Efremov D V and Eremin I 2008 *Phys. Rev. B* **78** 134512
[30] Cvetkovic V and Tesanovic Z 2009 *Phys. Rev. B* **80** 24512
[31] Richard P, Sato T, Nakayama K, Takahashi T and H D 2011 *Rep. Prog. Phys.* **74** 124512
[32] Nakayama K, Sato T, Richard P, Xu Y M, Sekiba Y, Souma S, Chen G F, Luo J L, Wang N L, Ding H and Takahashi T 2009 *Europhysics Lett.* **85** 67002
[33] Umezawa K, Li Y, Miao H, Nakayama K, Liu Z H, Richard P, Sato T, He J B, Wang D M, Chen G F, Ding H, Takahashi T and Wang S C 2012 *Phys. Rev. Lett.* **108**
[34] Liu Z H, Richard P, Nakayama K, Chen G F, Dong S, He J B, Wang D M, Xia T L, Umezawa K, Kawahara T, Souma S, Sato T, Takahashi T, Qian T, Huang Y B, Xu N, Shi Y B, Ding H and Wang S C 2011 *Phys. Rev. B* **84**
[35] Seo K J, Bernevig B A and Hu J P 2008 *Phys. Rev. Lett.* **101** 206404
[36] Fang C, Wu Y L, Thomale R, Bernevig B A and Hu J 2011 *Phys. Rev X* **1** 011009
[37] Si Q and Abrahams E 2008 *Phys. Rev. Lett.* **101** 76401
[38] Hu J and Ding H 2012 *Scientific Reports* **2** 381
[39] Hu J, Xu B, Liu W, Hao N and Wang Y 2012 *Phys. Rev. B* **85** 144403
[40] Lu X, Fang C, Tsai W F, Jiang Y and Hu J 2012 *Phys. Rev B* **85** 054505
[41] Berg E, Kivelson S A and Scalapino D J 2010 *Phys. Rev. B* **81** 172504
[42] Berg E, Kivelson S A and Scalapino D J 2009 *N. J. Phys.* **11** 085007
[43] Scalapino D J 1999 *Science* **284** 1282–1283
[44] de La Cruz C, Huang Q, Lynn J W, Li J, W Ratcliff I, Zarestky J L, Mook H A, Chen G F, Luo J L, Wang N L and Dai P 2008 *Nature* **453** 899–902
[45] Zhao J, Adroja D T, Yao D X, Bewley R, Li S L, Wang X F, Wu G, Chen X H, Hu J P and Dai P C 2009 *Nature Physics* **5** 555–560
[46] Dai P, Hu J and Dagotto E 2012 *Nature Physics* **In Press**
[47] Yi M, Lu D H, Analytis J G, Chu J H, Mo S K, He R H, Hashimoto M, Moore R G, Mazin I I, Singh D J, Hussain Z, Fisher I R and Shen Z X 2009 *Phys. Rev.B* **80** 174510
[48] Richard P, Nakayama K, Sato T, Neupane M, Xu Y M, Bowen J H, Chen G F, Luo J L, Wang N L, Ding H and Takahashi T 2010 *Phys. Rev. Lett* **104** 0909.0574
[49] Yi M, Lu D H, Chu J H, Analytis J G, Sorini A P, Kemper A F, Mo S K, Moore R G, Hashimoto M, Lee W S, Hussain Z, Devereaux T P, Fisher I R and Shen Z X 2011 *PNAS* **108** 6878
[50] Zhang Y, He C, Ye Z R, Jiang J, Chen F, Xu M, Ge Q Q, Xie B P, Wei J, Aeschlimann M, Cui X Y, Shi M, Hu J P and Feng D L 2012 *Phys. Rev. B* **85**

[51] Liu H and et a 2008 *Phys. Rev B* **78** 184514
[52] Liu G and et al. 2009 *Phys. Rev B* **80** 134519
[53] Ran Y, Wang F, Zhai H, Vishwanath A and Lee D H 2009 *Phys. Rev B* **79** 014505
[54] Lipscombe O J, Chen G F, Fang C, Perring T G, Abernathy D L, Christianson A D, Egami T, Wang N, Hu J and Dai P 2011 *Phys. Rev. Lett.* **106** 57004
[55] Wang M, Fang C, Yao D X, Tan G, Harriger L W, Song Y, Netherton T, Zhang C, Wang M, Stone M B, Tian W, Hu J and Dai P 2011 *Nature Comm.* **2** 580
[56] Putzke C, Coldea A I, Guillamn I, Vignolles D, McCollam A, Leboeuf D, Watson M D, Mazin I I, Kasahara S, Terashima T, Shibauchi T, Matsuda Y and Carrington A 2012 *Phys. Rev. Lett.* **108** 47002
[57] Tapp J H, Tang Z, Lv B, Sasmal K, Lorenz B, Chu P C W and Guloy A M A 2008 *Phys. Rev. B* **78** 60505
[58] Wang X C, Liu Q Q, Lv Y X, Gao W B, Yang L X, Yu R C, Li F Y and Jin C Q 2008 *Sol. Stat. Comm.* **148** 538
[59] Wang M, Wang M, Miao H, Carr S V, Abernathy D L, Stone M B, Wang X C, Xing L, Jin C Q, Zhang X, Hu J, Xiang T, Ding H and Dai P 2012 arXiv:1208.0909
[60] Zhang Y, Ye Z R, Ge Q Q, Chen F, Jiang J, Xu M, Xie B P and Feng D L 2012 *Nature Physics* **8** 371
[61] Qiu X, Zhou S Y, Zhang H, Pan B Y, Hong X C, Dai Y F, Eom M J, Kim J S, Ye Z R, Zhang Y, Feng D L and Li S Y 2012 *Phys. Rev. X* **2** 11010
[62] Fisher I R, Degiorgi L and Shen Z X 2011 *Rep. Prof. Phys.* **74** 124506
[63] Fang C, Yao H, Tsai W F, Hu J P and Kivelson S A 2008 *Phys. Rev. B* **77** 224509
[64] Xu C, Mller M and Sachdev S 2008 *Phys. Rev. B* **78** 20501
[65] Eremin I and Chubukov A V 2010 *Phys. Rev. B* **81** 24511
[66] Fernandes R M, Vanbebber L H, Bhattacharya S, Chandra P, Keppens V, Mandrus D, McGuire M A, Sales B C, Sefat A S and Schmalian J 2010 *Phys. Rev. Lett.* **105** 157003